PHYSICAL REVIEW C **86**, 014304 (2012)

The (^{3}He,t) reaction on ^{76}Ge, and the double-β-decay matrix element

J. H. Thies,[1] D. Frekers,[1] T. Adachi,[2] M. Dozono,[3] H. Ejiri,[4,5] H. Fujita,[4,6] Y. Fujita,[6] M. Fujiwara,[4] E.-W. Grewe,[1,*] K. Hatanaka,[4] P. Heinrichs,[1] D. Ishikawa,[4] N. T. Khai,[7] A. Lennarz,[1] H. Matsubara,[8] H. Okamura,[4,†] Y. Y. Oo,[9] P. Puppe,[1] T. Ruhe,[1,‡] K. Suda,[3] A. Tamii,[4] H. P. Yoshida,[10] and R. G. T. Zegers[11]

[1]*Institut für Kernphysik, Westfälische Wilhelms-Universität Münster, D-48149 Münster, Germany*

[2]*Research Center for Electron and Photon Science, Tohoku University, Sendai, Miyagi 982-0826, Japan*

[3]*RIKEN, 2-1, Hirosawa, Wako, Saitama 351-0198, Japan*

[4]*Research Center for Nuclear Physics, Osaka University, Ibaraki, Osaka 567-0047, Japan*

[5]*Nuclear Physics, Czech Technical University, Prague, Czech Republic*

[6]*Department of Physics, Osaka University, Toyonaka, Osaka 560-0043, Japan*

[7]*Center for Fundamental Research and Calculation, Institute for Nuclear Science and Technology, Hanoi, Vietnam*

[8]*Center for Nuclear Study, University of Tokyo, 7-3-1 Hongo, Bunkyo, Tokyo 113-0033, Japan*

[9]*Department of Physics, Mandalay University, Mandalay 05092, Myanmar*

[10]*CYRIC, Tohoku University, Aramaki, Aoba, Sendai 980-8578, Japan*

[11]*National Superconducting Cyclotron Laboratory, The Joint Institute for Nuclear Astrophysics and the Department of Physics and Astronomy, Michigan State University, East Lansing, Michigan 48824, USA*

(Received 18 March 2012; published 3 July 2012)

A ^{76}Ge(^{3}He,t)^{76}As charge-exchange experiment at an incident energy of 420 MeV has been performed with an energy resolution of 30 keV. The Gamow-Teller GT$^-$ strength distribution in ^{76}As, which is the intermediate nucleus in the double-beta ($\beta\beta$) decay of ^{76}Ge, has been extracted. An unusually strong fragmentation of the GT$^-$ strength is observed even at low excitation energies of $E_x \leqslant 5$ MeV. By combining the data with those for GT$^+$ transitions from a recent ^{76}Se(d,^{2}He)^{76}As measurement, the nuclear matrix element for the ^{76}Ge $2\nu\beta\beta$ decay has been evaluated. A lack of correlation among the GT transition strengths feeding the same levels from the two different directions is observed. The impact on the ^{76}Ge $2\nu\beta\beta$ decay nuclear matrix element is discussed.

DOI: 10.1103/PhysRevC.86.014304 PACS number(s): 25.55.Kr, 23.40.Hc, 27.50.+e

I. INTRODUCTION

Hadronic charge-exchange reactions of (p,n) and (n,p) types have been receiving increased importance as a tool to extract information about nuclear properties, which are directly connected to weak interaction processes [1–13] including those, which are relevant in nuclear astrophysics [14,15]. Important advancements have for instance been made towards the understanding of the nuclear matrix elements, which appear in the description of the nuclear double-beta ($\beta\beta$) decay. These are foremost a result of the high spectral resolution, which has been attained in charge-exchange reactions over the course of time [9–11].

The nuclear matrix element determines the $\beta\beta$ decay rate, and although nuclear charge-exchange reactions only give insight into its Gamow-Teller (GT) part, which is the one that drives the 2ν decay, charge-exchange reactions nevertheless provide much needed information for theoretical model builders, who are also concerned with the more complex description of the neutrinoless decay [16–28].

The present (^{3}He,t) charge-exchange study focuses on the $\beta\beta$ decaying nucleus ^{76}Ge. Owing to the high spectral resolution of order 30 keV, some remarkable features of this nucleus are being unveiled, which previous charge-exchange experiments at much lower resolution have been unable to identify [29]. Further, ^{76}Se(d,^{2}He)^{76}As data probing the GT$^+$ direction are available [10], which allow a rather complete reconstruction of the transition path of the $2\nu\beta\beta$ decay as being sketched in Fig. 1.

Several counting experiments have reported half-lives of the ^{76}Ge 2ν decay [30–38]. These have recently been examined by Barabash [39], who suggests a most likely value of $T^{(2\nu)}_{1/2} = (1.5 \pm 0.1) \times 10^{21}$ yr. Two initiatives for large-scale counting experiments, GERDA [40] and MAJORANA [41], are presently active to search for the neutrinoless decay, whereby the sensitivity will be significantly increased over the previous experiment described in Ref. [42], which already claimed its observation at the level of $2.23^{+0.44}_{-0.31} \times 10^{25}$ yr [43].

It may be useful to recall some of the basic features, which connect intermediate energy charge-exchange reactions to the $2\nu\beta\beta$ decay. In the most widely used approximation [46] the $2\nu\beta\beta$ half-life is given by

$$\frac{1}{T^{2\nu}_{1/2}} = G^{2\nu}(Q, Z)\left|M^{2\nu}_{\mathrm{DGT}}\right|^2, \tag{1}$$

where $G^{2\nu}(Q, Z)$ is the phase-space factor depending on the decay Q value and the atomic charge Z of the nucleus. The

*Present address: RWE Vertrieb AG, Structuring, and Hedging, Dortmund, Germany.

†Deceased.

‡Institut für Experimentelle Physik 5b, Technische Universität, D-44221 Dortmund, Germany.

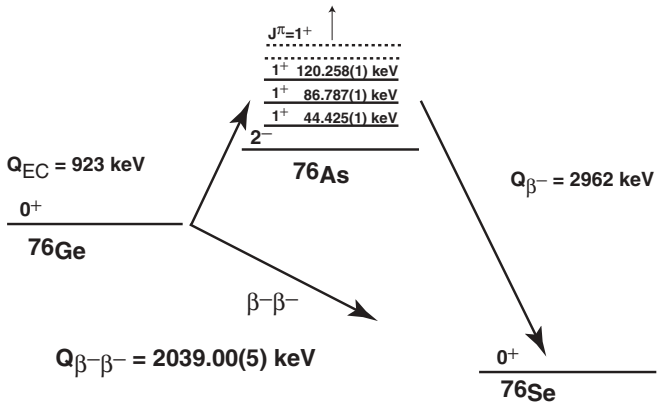

FIG. 1. Sketch of the $\beta\beta$ decay process of ^{76}Ge. The $2\nu\beta\beta$ transition path through the intermediate 1^+ states in ^{76}As is indicated. The Q values and excitation energies are taken from Refs. [44,45].

$2\nu\beta\beta$ decay "double GT" matrix element

$$M^{2\nu}_{\mathrm{DGT}} = \sum_m \frac{M_m(\mathrm{GT}^+)\cdot M_m(\mathrm{GT}^-)}{\frac{1}{2}Q + E_x(1^+_m) - E_0} \tag{2}$$

is the sum of two consecutive single β decay matrix elements, each of GT type, between the initial and an intermediate state and between that intermediate state and the final state. Since the GT operator $(\vec{\sigma}\cdot\vec{\tau})$ has no spatial dependence, the matrix element describes a $0^+ \rightarrow 1^+ \rightarrow 0^+$ decay path for a $0^+ \rightarrow 0^+$ initial to final ground-state to ground-state transition. The energy denominator in Eq. (2) contains the Q value of the decay and the energy difference $[E_x(1^+_m) - E_0]$ between the m^{th} intermediate 1^+ state and the initial ground state. The fourth-power dependence on the weak axial-vector coupling constant g_A is included in $G^{2\nu}(Q, Z)$.

The single β decay matrix element relates to the observable GT transition strength through

$$B_m(\mathrm{GT}^\pm) = |M_m(\mathrm{GT}^\pm)|^2 \tag{3}$$

for an initial ground-state spin-zero target. The GT^+ and GT^- transitions are selectively and strongly excited in hadronic (n,p)- and (p,n)-type reactions at intermediate energies and at low momentum transfers. This is a direct consequence of the dominant $V_{\sigma\tau}$ component of the effective nucleon-nucleon (NN) interaction at medium energies [47,48]. This interaction is embedded in most distorted wave (DW) reaction calculations, which allow a rather straightforward extraction of the relevant B(GT) strength values from the experimental data. One may also note that Fermi transitions to the isobaric analog states are mediated by the V_τ interaction component, however, because of isospin selection rules, these transitions are only allowed for (p,n)-type reactions.

The present experiment follows this scheme by using the $(^3\mathrm{He},t)$ reaction as a high-resolution alternative to the elementary (p,n) probe [49–51]. However, one should note that despite the high selectivity of charge-exchange reactions, these are not primarily intended to compete with counting rates experiments on evaluating half-lives. Further, although the individual $\beta\beta$ decay matrix elements appearing in Eq. (2) can be readily evaluated by combining GT^+ and GT^- transition strengths, sign properties, which may be important for their summation, get lost because of Eq. (3). Charge-exchange reactions, on the other hand, provide a unique and detailed insight into the individual properties of a nucleus, and ^{76}Ge is a prime example of the potentially complex and rather unexpected structure of nuclear matrix elements in $\beta\beta$ decay.

II. EXPERIMENT

The experiment was performed at the Research Center for Nuclear Physics (RCNP), Osaka University. A 420 MeV $^3\mathrm{He}^{++}$ beam was accelerated using the Azimuthally Varying Field (AVF) Cyclotron in combination with the Ring Cyclotron and transported to the scattering chamber of the Grand Raiden Spectrometer (GRS) [52]. The WS beam line [53] provided the necessary beam dispersion for achieving high resolution. Several tuning techniques for the dispersion matching between beam-line and spectrometer were employed to optimize the energy and angular resolutions. The details are described in Refs. [52–56].

Outgoing reaction tritons were momentum analyzed in the Grand Raiden Spectrometer within its full acceptance of ± 20 mrad in horizontal and ± 40 mrad in vertical direction. Depending on the angular setting, the primary beam was stopped by a Faraday cup either inside the first dipole magnet or inside the first quadrupole magnet.

The detection system consisted of a set of two multiwire drift chambers (MWDC) each with a X/U arrangement, which allowed precise track reconstruction on the focal plane [57]. They were followed by two thin (3 and 10 mm) plastic scintillators used for particle identification and for providing the trigger signals.

A thin self-supporting germanium target was used. Its areal thickness was determined by performing energy-loss measurements of α particles traversing the target foil in a specially designed setup. In the present case the α-source employed contained the three radio-isotopes ^{239}Pu, ^{241}Am, and ^{244}Cm, which feature three strong decay branches at 5.154 MeV (^{239}Pu), 5.486 MeV (^{241}Am), and 5.805 MeV (^{244}Cm). The thickness from these energy-loss measurements was calculated using the computer code SRIM [59] and determined to be 1.43(4) mg/cm^2. With this target thickness and after applying various off-line spectrometer aberration corrections (up to a tenth order polynomial), an energy resolution of $\approx$30 keV was obtained.

The Ge material was isotopically enriched and specified as 86% ^{76}Ge with the remaining percentage being mostly ^{74}Ge. The superb spectral resolution of the $(^3\mathrm{He},t)$ experiment allowed an analysis of the cross-section yields from the different isobaric analog states (cf. Fig. 2), whose Fermi transition strengths are given by $B(\mathrm{F}) = (N - Z)$. These yields mirror the isotopic composition of the target. A detailed search for isobaric analog states from the other stable isotopes (^{70}Ge, ^{72}Ge, and ^{73}Ge) revealed traces of an analog transition in ^{72}Ge and in ^{70}Ge. The transition energies and the identified isotopic percentages analyzed in this way are listed in Table I. A possible contribution from ^{73}Ge could not be identified since its transition is masked by the IAS of ^{74}Ge. After the completion of the experiment a small target sample

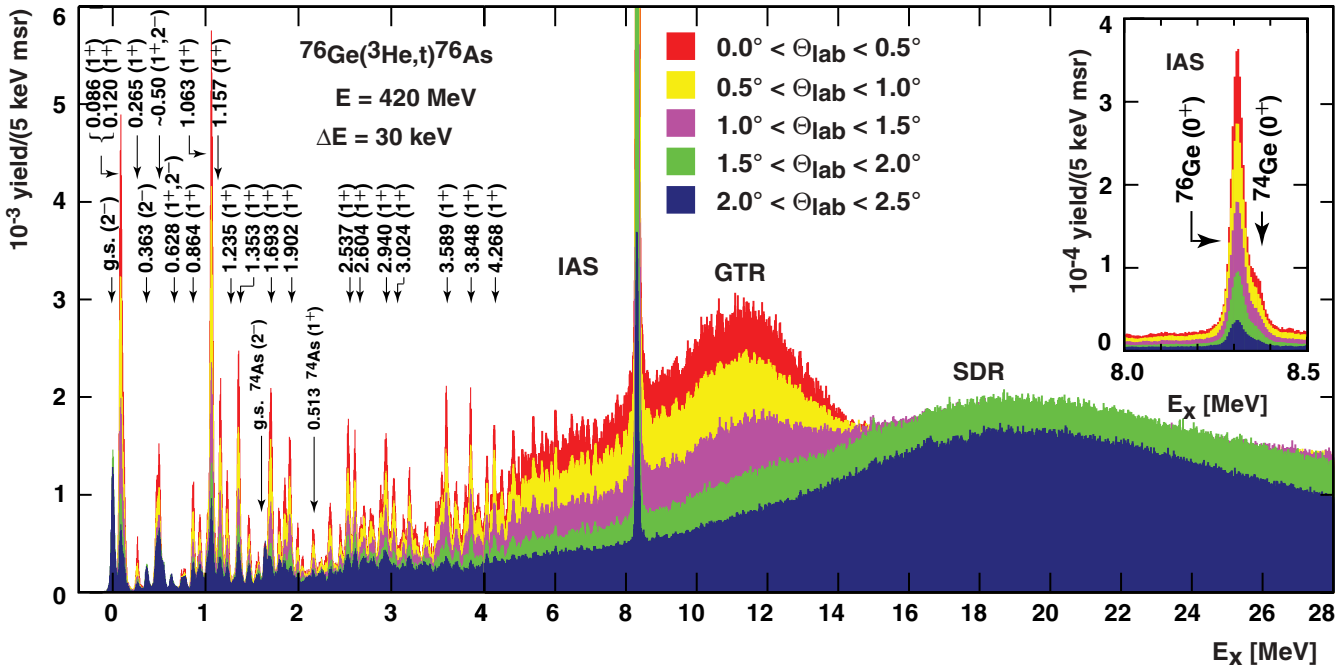

FIG. 2. (Color) Excitation-energy spectra for the ^{76}Ge(^{3}He,t)^{76}As reaction. The spectra were generated from different angle cuts (as indicated by the colors) and stacked on top of each other to indicate the effect of the angular dependence. Transitions with $\Delta L = 0$ are forward peaked and appear in red at the most forward angle. Note, the energy scale is compressed above 4 MeV. The various states with their spin assignments are indicated. The GT resonance (GTR) and the spin-dipole resonance (SDR) are centered at ≈11 MeV and ≈18.5 MeV. The inset shows the isobaric analog states at 8.308 MeV (from ^{76}Ge) and 8.360 MeV (from ^{74}Ge, which corresponds to 6.721 MeV in the excitation frame of ^{74}As).

was independently analyzed for its isotopic composition at the Gran Sasso National Laboratory (LNGS) [58] by using the high-precision technique of inductively coupled plasma-mass spectrometry (ICP-MS). The measured percentages of the isotopic composition of the Ge-target are also listed in Table I. Both methods give consistent results.

An energy calibration at the level of ±1 keV precision for the low excitation-energy region (i.e., below the IAS) was performed with a ^{26}Mg and a ^{nat}Si target. The (^{3}He,t) spectra on these targets provide numerous discrete levels with well-known excitation energies distributed over a large momentum bite in the focal plane. One may note that in the excitation-energy region below ≈2 MeV, the extracted states match those from the Brookhaven National Nuclear Data Center (NNDC) database [60] with remarkable precision (cf. Table III).

The experiment was performed at two spectrometer-angle settings, i.e., 0° and 2.5°. Appropriate solid angle cuts allowed generating angular distributions ranging from about 0° to 4.0°.

TABLE I. Isotopic composition of the Ge target deduced from the strength of the isobaric analog transitions in the ^{76}Ge(^{3}He,t)^{76}As spectrum (mass dependent corrections included) and from a direct measurement using the ICP-MS technique. IAS excitation energies are quoted in the ^{76}As excitation frame (column one) and in the excitation frames of the daughter nuclei ($^{70+x}$As, $x = 0, 2, 3, 4, 6$) (column two).

Isotope	$E_x(^{76}\text{As})$	$E_x(^{70+x}\text{As})$	B(F)	IAS	ICP-MS Ref. [58]
^{76}Ge	8.308	8.308	12	86.8(8)%	86.9(1)%
^{74}Ge	8.360	6.721	10	12.2(9)%	11.83(8)%
^{73}Ge	–	–	9		0.249(2)%
^{72}Ge	8.456	5.023	8	0.75(12)%	0.583(4)%
^{70}Ge	8.505	3.208	6	0.25(13)%	0.384(5)%

III. DETAILED ANALYSIS

A set of ^{76}Ge(^{3}He,t)^{76}As spectra at five different forward scattering angles is shown in Fig. 2. The spectra have been arranged in such a way that the most forward-angle spectrum appears in the back and the others are stacked on top of each other using different color codings. This way the angular dependence of the various components can be quickly identified, e.g., forward-peaked cross sections are likely GT transitions (colored red) with angular momentum transfer $\Delta L = 0$ and more backward peaked ones are likely $\Delta L = 1$ spin-dipole transitions (colored blue/green).

The spectra show an extraordinary large number of isolated states up to ≈5 MeV excitation energy followed by the strongly excited IAS of ^{76}Ge at $E_x = 8.308$ MeV with a shoulder from the IAS of ^{74}Ge at $E_x = 8.360$ MeV. Around $E_x = 11$ MeV one observes the peak of the GT resonance (GTR) and at about 18.5 MeV the rather broad ($\Gamma \simeq 10$ MeV) spin-dipole resonance (SDR). The spectra are qualitatively similar to the ones reported by Madey *et al.* [29] from a (p,n) measurement at 134.4 MeV, although those were generated at a much reduced resolution of order 380 keV.

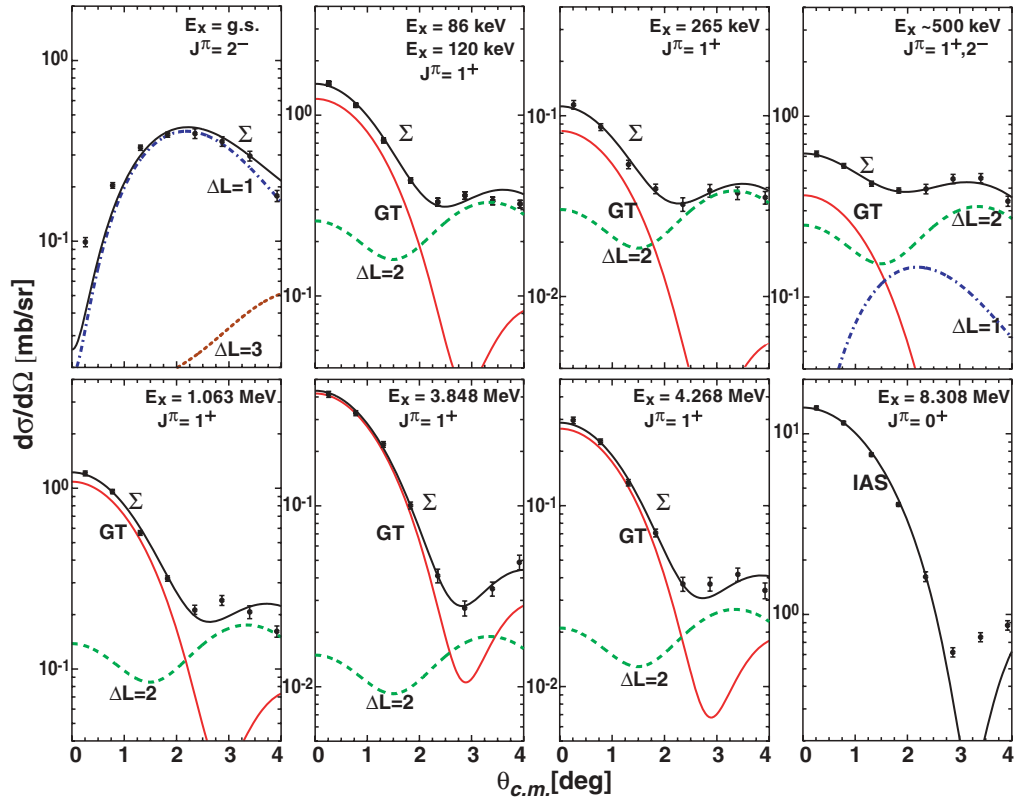

FIG. 3. (Color) Cross-section angular distributions for selected states of the ^{76}Ge(^{3}He,t)^{76}As reaction as discussed in the text. Note that the states around 100 keV and 500 keV could not be separated. The data points represent their sum.

With the present energy resolution of 30 keV (FWHM) more than 70 individual states (most of them 1^+ states), can be resolved below 5 MeV. For all of these an angular distribution has been generated, by which definitive spin assignments are given. For instance, the ^{76}As ground state (g.s.) is clearly resolved and the $\Delta L = 1$ type angular distribution supports the 2^- assignment (cf. Figs. 2 and 3). A triplet of 1^+ states is known at 44.4, 86.8, and 120.3 keV [60]. However, in the present (^{3}He,t) spectrum there is no firm indication for a transition to the 44.4 keV level. From the two remaining states the lower one at 86.8 keV is the most strongly excited, which makes disentangling the two states over the full angular range difficult. An angular distribution was therefore generated from the sum of the two states (see Fig. 3). A similar procedure was followed for the states at around 500 keV.

Above $E_x \approx 2$ MeV, the level density increases rapidly, and peak identification relies increasingly on peak-fitting procedures, for which Gaussian-peak profiles at a fixed width have been used. This technique is followed to about 5 MeV excitation. As already mentioned, the excitation energies extracted by this procedure are in excellent agreement with those given in the NNDC database [60].

In the ^{76}Ge excitation frame the ^{74}As ground state ($J^\pi = 2^-$) from the (^{3}He,t) reaction on the ^{74}Ge contaminant can be reasonably well identified in the spectra in Fig. 2 at $E_x = 1.637$ MeV. The intensity ratio to the ^{76}As($J^\pi = 2^-$) g.s. transition mirrors the isotopic ratio. However, there is no clear indication for a sizable excitation to the first known $J^\pi = 1^+$, 206.6 keV state, which should appear at $E_x = 1.846$ MeV. Instead, we attribute the state at 1.852 MeV (cf. Table III) to a genuine state in ^{76}As at 1.849(10) MeV. The second known $J^\pi = 1^+$ state at 422.2 keV in ^{74}As should appear at 2062.4 keV. Again, we do not see any indication for its excitation. The next known $J^\pi = 1^+$ state at 513.8 keV in ^{74}As [60] should be located at 2.153 MeV. In this case we attribute the state identified with $J^\pi = 1^+$ at 2.154 MeV to that state, whose B(GT) value would then be relatively large at $\approx$0.1 (cf. Table III). In the following analysis, transitions above this energy of 2.154 MeV will still be treated as originating from the ^{76}Ge(^{3}He,t) reaction, which is a sensible assumption for the most strongly excited states. These are those, which appear in Fig. 2 labeled by their excitation energies. However, when evaluating summed B(GT) strengths or nuclear matrix elements, we assume on average a 14% reduction (according to isotopic abundance) of the $B(\mathrm{GT}^-)$ values for all states above 2.154 MeV.

The data taken at the two angle settings of the spectrometer, i.e., 0° and 2.5°, were sorted into five, respectively, four angle bins, which are [0° − 0.5°], [0.5° − 1.0°], [1.0° − 1.5°], [1.5° − 2.0°], [2.0° − 2.5°] and [2.0° − 2.5°], [2.5° − 3.0°], [3.0° − 3.5°], [3.5° − 4.0°]. The various software cuts may induce an extra systematic error on the final cross section, which we assume of order 2% for the 0° setting and about 5% for the 2.5° setting.

TABLE II. Optical model parameters used for the ^{76}Ge(^{3}He,t) reaction calculation.

Projectile / ejectile	V_R (MeV)	r_R (fm)	a_R (fm)	W_I (MeV)	r_I (fm)	a_I (fm)
^{3}He	− 34.67	1.33	0.825	− 54.17	0.991	1.056
^{3}H	− 29.47	1.33	0.825	− 46.04	0.991	1.056

A. DWBA calculations

A set of angular distributions is shown in Fig. 3 and compared with DWBA calculations performed with the codes NORMOD [61] and FOLD [62].

In the FOLD code, the effective NN interaction developed by Love and Franey [47,48] is double-folded over the transition densities. Components of the interaction such as the central part, spin-orbit and tensor are included and the exchange part is treated in the short-range approximation as described in Refs. [47,63].

The program NORMOD [61] was used to determine the one-body transition densities (OBTD). The single-particle wave functions were generated by Woods-Saxon potentials with a radius of $r_0 = 1.25$ fm and a diffuseness parameter $a = 0.5$ fm [64]. The Coulomb radius was set to $r_C = 1.25$ fm.

The distortion of the incoming and outgoing waves was treated in an optical model (OM). Appropriate OM parameters were adapted from ^{90}Zr and ^{58}Ni quoted in Ref. [65]. Since there are no OM parameters available for tritons, potential depth parameters for the outgoing tritons were set to 85% of those for ^{3}He following the recipe of Ref. [66]. We note that the B(GT) values extracted from the cross sections near zero momentum transfer are rather robust against variations of the OM parameters to within reasonable bounds. The OM parameters are listed in Table II.

In order to obtain a good description of the experimental angular distributions, we find that for most of the 1^+ states there is a need to add some sizable $\Delta L = 2$ angular momentum transfer component to reproduce the cross-section data. A similar need was also reported in Ref. [67] for a much heavier system, where it seemed to be even more pronounced. The component should add coherently to the cross section, however, due to the lack of a realistic wave function, one is simply left to add it in an incoherent way.

Angular distributions for selected transitions with $J^\pi = 0^+$ (IAS), 1^+, and 2^- (g.s.) are shown in Fig. 3.

B. Determination of the Gamow-Teller strength

There are various ways to extract the GT strength from the angular distribution. All of them relate the GT part of the cross section to the weak decay by extrapolating the angular distribution to zero momentum transfer ($q = 0$). The functional form of this extrapolation can be approximated by the zeroth order Bessel function $|j_0(qR_0)|^2$ with R_0 being the interaction radius (see, e.g., Ref. [7]). This extrapolation is in accord with the standard plane-wave approach and may not be an appropriate description for the hadronic reaction, as this requires the matching between incoming and outgoing distorted Coulomb waves. Thus, following Ref. [7]:

$$\left.\frac{d\sigma^{GT}}{d\Omega}\right|_{(q=0)} = \left(\frac{\mu}{\pi\hbar^2}\right)^2 \frac{k_f}{k_i} N_D^{\sigma\tau} |J_{\sigma\tau}|^2 B(\mathrm{GT}), \qquad (4)$$

where $J_{\sigma\tau}$ is the volume integral of the effective interaction [47] and $N_D^{\sigma\tau}$ the OM distortion factor defined as the ratio of the distorted (DW) and plane wave (PW) cross sections [7]:

$$N_D^{\sigma\tau} = \frac{\sigma_{DW}(q=0)}{\sigma_{PW}(q=0)}. \qquad (5)$$

With the present OM parameters we calculate $N_D^{\sigma\tau} = 0.0633$, which compares to within 3% to the functional form given in Ref. [68]. In Ref. [69] a rather precise value of 161.5 MeV·fm^3 for $J_{\sigma\tau}$ was extracted for mass $A = 71$.

A set of angular distributions is shown in Fig. 3 with the various extracted GT parts indicated. Because of the uncertainty, with which the non-GT contribution can be evaluated at $q = 0$, we assume that 50% of the non-GT part to the cross section at $q = 0$ should enter into the error calculation for the GT strength values. Such a conservative error margin would then also include possible non-GT tensor contributions to the cross section. We do, however, observe that above 4 MeV excitation, i.e. on the low-energy tail of the GTR, the non-GT part of the individual states decreases significantly, which may be interpreted as a result of a stronger coupling of the individual states to the giant resonance.

The B(GT) strength values for most of the transitions up to ≈5 MeV extracted in this way are listed in Table III. The integrated yield gives a value of $\sum_{0-5\mathrm{MeV}} B(\mathrm{GT}) = 1.48$, which includes the average 14% reduction of all B(GT) values above 2.154 MeV discussed earlier. The B(GT) running sum is shown in Fig. 5.

The present analysis of the B(GT) distribution and the running sum is based on individual, well separated transitions as shown in Fig. 2. However, with increasing excitation energy there may be an increased contribution to the B(GT) strength unaccounted for, which is mainly a result of the rather structureless low-energy tail of the GTR. A consistency check has therefore been performed by extracting B(GT) strength values from angular distributions generated for ten narrow energy bins of 0.5 MeV and two rather wide energy bins of 2.5 MeV width from 0–5 MeV excitation energy. The extraction procedure is identical to the one described earlier for individual states. The relevant angular distributions are shown in Fig. 4. The B(GT) values summed over each 0.5 MeV energy bin are shown as open circles in Fig. 5 showing that the different approaches give consistent results. Further, above ≈3 MeV excitation the background contribution from the GTR starts to become significant, as expected. The numerical values are listed in Table IV. We also note that the extracted summed B(GT) values are in good overall agreement with those given by Madey *et al.* [29] from the rather low resolution (p,n) measurement.

C. Extraction of $2\nu\beta\beta$ decay matrix elements

For the evaluation of the $2\nu\beta\beta$ decay matrix elements a one-to-one connection to the $B(\mathrm{GT}^+)$ transitions leading

TABLE III. Excitation energies, cross sections, B(GT) values ($\times 10$) for low-lying states populated through the ^{76}Ge(^{3}He,t)^{76}As reaction (left and right table). In column one, excitation energies from Ref. [60] (spins quoted if known, errors quoted if significant) are compared with those from the (^{3}He,t) reaction in column three (errors ± 1 keV). Column five lists cross sections at $q = 0$, and column six their GT fraction. B(GT) values appear in column seven. Cross-section errors are statistical ones only. Errors for B(GT) values include an extra 50% contribution from the non-GT part of the cross section at $q = 0$. In a few cases the errors exceed 100%, which is unphysical. We have nonetheless followed the prescription for clarity. The spin assignments in square brackets indicate the presence of two closely spaced and unresolved states of different spins analyzed as indicated. The 471 and 500 keV transition yields were summed in the analysis. Note, the state at 2.154 MeV in the ^{76}As excitation frame is likely a 1^+ state in ^{74}As at 513.8 keV (cf. appropriate line in this table). Its B(GT) strength has been excluded in the following analyses. For the summed B(GT) we have quoted the full and the 14% reduced values.

^{76}As (Ref. [60])		^{76}As		$\frac{d\sigma}{d\Omega}(q=0)$	GT	B(GT)	^{76}As [60]		^{76}As		$\frac{d\sigma}{d\Omega}(q=0)$	GT	B(GT)
E_x[keV]	J^π	E_x[keV]	J^π	[mb/sr]	%	$\times 10$	E_x[keV]	J^π	E_x[keV]	J^π	[mb/sr]	%	$\times 10$
0	2^-	0	2^-	–	–	–			2763	1^+	0.099(2)	64	0.08(2)
86.8	$(1)^+$	86	1^+	1.173(19)	83	1.20(13)			2791	1^+	0.133(3)	86	0.14(1)
120.3	$(1)^+$	120	1^+	0.318(7)	83	0.33(3)			2819	1^+	0.069(2)	47	0.04(2)
264.8	$(1, 2)^+$	265	1^+	0.113(3)	73	0.10(2)			2882	1^+	0.193(4)	82	0.20(2)
363.9	$(1^-, 2^-)$	363	2^-	–	–	–			2918	1^+	0.107(3)	84	0.11(1)
471/500	$(1^+, 2^+)$	≈500	$[1^+, 2^-]$	0.621(10)	59	0.45(16)			2940	1^+	0.354(7)	85	0.37(3)
628.7	$(1, 2, 3^-)$	628	$[2^-, 3^+]$	0.039(1)	15	0.01(2)			3024	1^+	0.238(5)	89	0.26(2)
745.0	$(1^+, 2^+)$	744	$[1^+, 3^+]$	0.059(1)	23	0.02(3)			3134	$[1^+, 2^-]$	0.120(3)	82	0.12(1)
774.4	$(1, 2, 3)^+$	774	$[1^+, 3^+]$	0.067(2)	20	0.02(3)			3190	$[1^+, 2^-]$	0.254(5)	87	0.27(2)
863.4	$(1, 2, 3)^+$	864	1^+	0.284(7)	72	0.25(5)			3257	1^+	0.097(2)	73	0.09(2)
935.4	$\leqslant 3$	936	1^+	0.209(5)	70	0.18(4)			3364	$[1^+, 2^-]$	0.070(2)	64	0.06(2)
1023.2	$(1^+, 2^+)$	1022	$[1^+, 3^+]$	0.275(4)	52	0.18(8)			3426	2^-	–	–	–
1064.5	$(1^+, 2^+)$	1063	1^+	1.230(20)	89	1.36(9)			3482	1^+	0.107(3)	83	0.11(1)
1097.3	$\leqslant 3$	1098	1^+	0.157(4)	79	0.15(2)			3504	1^+	0.062(3)	89	0.07(1)
1156.6		1157	1^+	0.495(10)	90	0.56(3)			3540	1^+	0.230(5)	88	0.25(2)
1230(10)		1235	1^+	0.298(6)	75	0.28(5)			3589	1^+	0.421(9)	91	0.48(2)
1352.4	$\leqslant 3$	1353	1^+	0.615(11)	81	0.62(7)			3634	1^+	0.106(3)	80	0.11(1)
1473.7	$\leqslant 3$	1475	1^+	0.260(5)	64	0.21(6)			3695	1^+	0.227(5)	85	0.24(2)
1541.7	$\leqslant 3$	1540	$[1^+, 3^+]$	0.069(2)	34	0.03(3)			3798	1^+	0.181(5)	95	0.21(1)
1571.3	$\leqslant 3$	1573	$[1^+, 2^-]$	0.071(2)	98	0.09(1)			3848	1^+	0.441(10)	97	0.53(1)
1638.0	$\leqslant 3$	1637	$[1^+, 2^-]$[a]	0.099(2)	27	0.03(4)			3932	1^+	0.186(5)	93	0.22(1)
1639.5(2)	^{74}As, 2^-	0	2^-	–	–	–			4034	1^+	0.119(3)	87	0.13(1)
1694.6	$\leqslant 3$	1693	1^+	0.451(9)	88	0.49(3)			4071	1^+	0.239(6)	91	0.27(1)
1715.6	$\leqslant 3$	1718	1^+	0.125(3)	84	0.13(4)			4109	1^+	0.052(1)	66	0.04(1)
1794.6	$\leqslant 3$	1792	1^+	0.159(3)	64	0.13(4)			4179	1^+	0.103(3)	92	0.12(1)
1849(10)		1852	1^+	0.326(6)	82	0.33(4)			4218	1^+	0.116(4)	95	0.14(1)
		1902	1^+	0.379(9)	96	0.45(1)			4268	1^+	0.294(7)	93	0.34(1)
1928(10)		1929	$[1^+, 2^-]$	0.044(1)	76	0.04(1)			4306	1^+	0.187(4)	89	0.21(1)
1988(10)		1987	1^+	0.094(2)	82	0.10(1)			4466	1^+	0.094(3)	83	0.10(1)
2032(10)		2041	1^+	0.053(2)	98	0.06(1)			4499	1^+	0.167(4)	92	0.19(1)
2147(10)	$\rightleftharpoons$	2154	1^+	0.125(3)	77	0.12(2)			4536	1^+	0.055(2)	94	0.06(1)
2153(2)	^{74}As(1^+)	513.8	1^+	0.725(17)	77	0.71(10)			4668	1^+	0.046(1)	76	0.04(1)
2338(10)		2338	1^+	0.184(4)	83	0.19(2)			4699	1^+	0.153(6)	100	0.19(1)
2446(10)		2449	1^+	0.111(3)	67	0.09(2)			4738	1^+	0.137(4)	91	0.16(1)
		2537	1^+	0.377(7)	87	0.41(3)			4801	1^+	0.261(6)	92	0.30(1)
		2604	1^+	0.347(7)	76	0.33(5)			4841	1^+	0.234(6)	97	0.28(1)
		2657	1^+	0.096(2)	69	0.08(2)			4941	1^+	0.101(3)	94	0.12(1)
		2688	1^+	0.122(3)	83	0.13(1)			4978	1^+	0.151(4)	87	0.16(1)
		2716	1^+	0.126(3)	60	0.09(3)						$\sum =$	16.0(18)
													14.8(17)

[a]Composed of a ^{76}As 1^+ state and the ^{74}As 2^- g.s. (next line)

to the same levels in the intermediate nucleus according to Eq. (1) needs to be established. Rather detailed experimental information is available from the ^{76}Se(d,^{2}He)^{76}As reaction performed at the Kernfysisch Versneller Instituut (KVI), Groningen, with a 183 MeV incident deuteron beam and a resolution of 120 keV [10]. In Fig. 6 the spectra from the two sides, both taken near zero degree, are shown. The two spectra show a remarkable lack of correlation, which was something

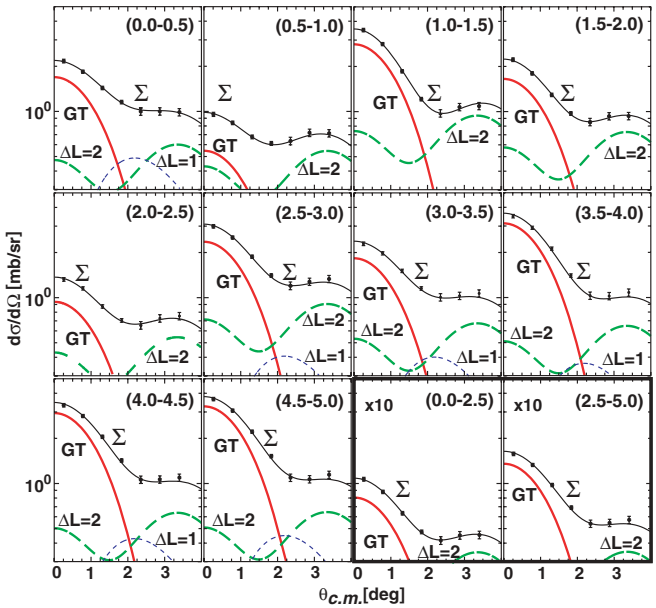

FIG. 4. (Color) Cross-section angular distributions generated from ten $\Delta E = 0.5$ MeV and two $\Delta E = 2.5$ MeV energy bins (lower right) compared with DW model calculations. Extracted B(GT) values are listed in Table IV.

already noticed in Ref. [10] when comparing the (d,^{2}He) data with the earlier low-resolution (p,n) data from Madey *et al.* [29]. Whereas the GT$^+$ strength is mostly concentrated in five relatively strong states, the GT$^-$ strength is fragmented into many states. For instance, above 1 MeV no single state carrying a major fraction of GT$^-$ strength exists, unlike the situation on the GT$^+$ side. The following detailed inspection also reveals that there seems to be an anticorrelation among the transitions from the two directions, which is something also observed in the mass $A = 48$ case [9]. Strong transitions from one direction do not seem to have a strong partner from the other direction and vice versa.

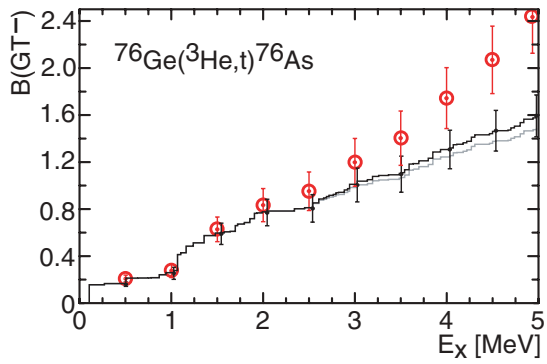

FIG. 5. (Color online) Running sum of the B(GT) strength from individual ^{76}Ge(^{3}He,t) transitions. The grey curve indicates the result after a 14% reduction of all B(GT) values above 2.154 MeV owing to the 14% ^{74}Ge content of the target. The circles indicate the extracted values over 0.5 MeV energy bins, showing above ≈3 MeV the increasing influence of the GTR.

TABLE IV. B(GT) strength values extracted from 0.5 MeV energy bins and compared with those of individual states summed over the same energy bins. The bottom part shows the analysis for 2.5 MeV energy bins. Above 2.2 MeV the 14% reduction of extracted B(GT) values is incorporated.

^{76}As E_x [MeV]	%GT	B(GT) $\Delta E = 0.5$ MeV	B(GT) indiv. states
0.0–0.5	77	0.210(31)	0.163(18)
0.5–1.0	55	0.068(27)	0.093(33)
1.0–1.5	79	0.351(47)	0.335(39)
1.5–2.0	74	0.207(37)	0.182(22)
2.0–2.5	68	0.118(23)	0.035(04)
2.5–3.0	76	0.255(40)	0.199(27)
3.0–3.5	77	0.199(30)	0.092(09)
3.5–4.0	86	0.341(29)	0.210(11)
4.0–4.5	85	0.323(29)	0.154(09)
4.5–5.0	86	0.360(29)	0.136(05)
	$\sum_{0-5\text{MeV}}$	= 2.43(32)	$\sum_{0-5\text{MeV}}$ = 1.60(18)
0–2.5	73	0.95(18)	
2.5–5.0	84	1.49(15)	
	$\sum_{0-5\text{MeV}}$	= 2.45(32)	

In an initial attempt those transitions, which are clearly identifiable from both directions, are used to form the $\beta\beta$ decay matrix element of Eq. (2). Since the spectra from the two charge-exchange experiments feature rather different energy resolutions, one is forced to combine states within the ≈120 keV resolution bin of the (d,^{2}He) reaction and take the sum of their GT$^-$ strengths to evaluate the matrix element. This is certainly a reasonable approach as long as the states within these energy bins are not strongly anticorrelated. In a few cases the energy bin was slightly extended in order to generously accommodate the peak tail areas from the (d,^{2}He) side (see, e.g., Fig. 7). The individual values are listed in Table V. The summed matrix elements reach a value of $\sum M^{2\nu}_{\text{DGT}} = 0.186 \pm 0.016$ MeV^{-1}.

To estimate possible contributions from those states on the (^{3}He,t) side, which have no obvious partner on the (d,^{2}He) side, an attempt was made to correlate the states observed between 2–5 MeV in the (^{3}He,t) reaction with the possible GT continuum background contribution observed in the (d,^{2}He) case. The integrated GT strength of the (d,^{2}He) reaction in the continuum above 2.5 MeV was analyzed in Ref. [10] to be of order $B(\text{GT}^+) = 0.15$, however with a large uncertainty, which also makes this contribution compatible with zero. This strength has been evenly distributed over the 2–5 MeV energy region in bins of $\Delta E = 30$ keV as indicated in Fig. 7. The additional contribution to the matrix element then amounts to 0.048 MeV^{-1}, yielding a total value of $\sum M^{2\nu}_{\text{DGT}} = 0.23$ MeV^{-1}. Because of the uncertainty of the continuum background strength, it may be justified to place an error margin of $\Delta M^{2\nu}_{\text{DGT}} = 0.07$ MeV^{-1} to this value.

The data situation certainly limits any further-reaching conclusions. Nevertheless, it is interesting to note that the GT transitions to the low-excitation region make up most of the $2\nu\beta\beta$ decay matrix elements. In fact, an evaluation of the

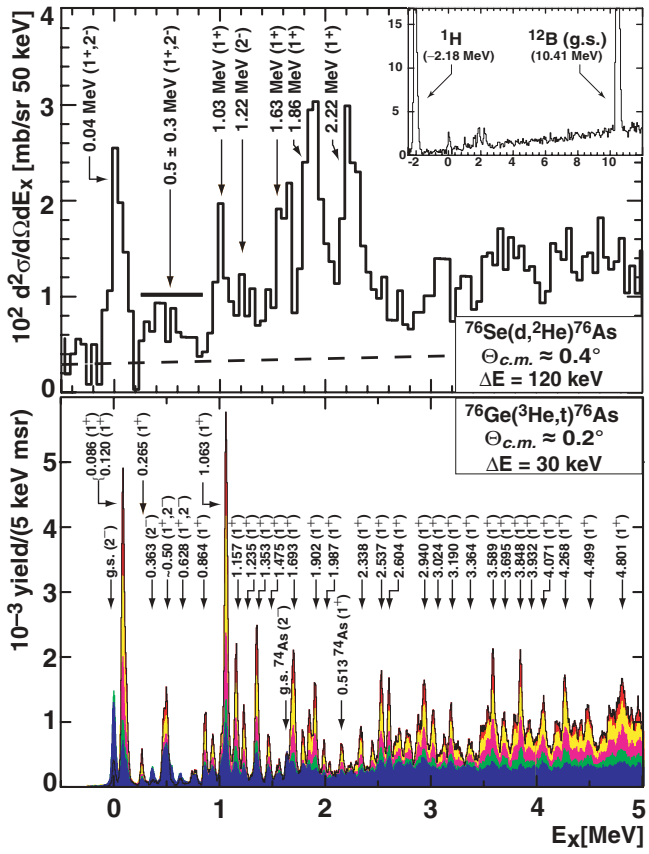

FIG. 6. (Color) Comparison of the ^{76}Se(d,^{2}He)^{76}As spectrum (from Ref. [10]) with the one from the ^{76}Ge(^{3}He,t)^{76}As reaction. The color coding for the lower spectra is the same as in Fig. 2. The dashed line in the ^{76}Se(d,^{2}He)^{76}As spectrum indicates the level of instrumental background. The inset shows the excitation spectrum up to 12 MeV and the ^{12}C(d,^{2}He)^{12}B(g.s.) reaction from the carbon backing of the target. The hydrogen line is an ever present background line in metallic targets.

matrix element from the half-life quoted by Barabash [39] and using the phase-space factor given in Ref. [18] modified by the most recent value of the unquenched axial-vector coupling constant of $g_A = -1.2694$ [70] one arrives at $M^{2\nu}_{\rm DGT} = 0.137(4)\text{MeV}^{-1}$, which is even smaller than any of the matrix elements quoted above. This is surprising, as it suggests that any further GT$^\pm$ contributions unaccounted for, notably those from the GTR, are either small [71,72] or they effectively cancel by phase cancelation [73], or alternatively, the anticorrelation among the states from the two reaction directions is more pronounced than so far assumed. Experimentally, there is indeed evidence for a severe lack of correlation among the three lowest-lying 1^+ states at 44.4, 86.8, and 120.3 keV. In the (d,^{2}He) reaction the 44.4 keV state seems to be strongly excited with little strength appearing at 120.3 keV, whereas the (^{3}He,t) transition strength is clearly more concentrated at 86.8 and 120.3 keV with almost no strength at 44.4 keV. The matrix element, which has so far been evaluated from these three states, contributes ≈30% to the total value, and an anticorrelation could reduce this number significantly.

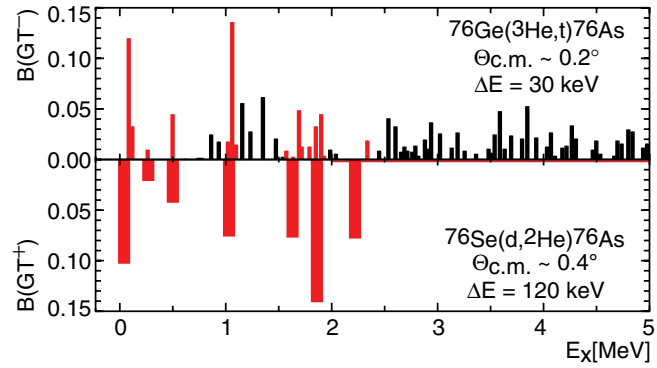

FIG. 7. (Color) B(GT$^\pm$) strength distribution from the ^{76}Se(d,^{2}He)^{76}As [10] and ^{76}Ge(^{3}He,t)^{76}As reactions. The width of the bars indicate the energy resolution. Correlated states are indicated by red bars. Above 2 MeV the possible B(GT$^+$) continuum contribution quoted in Ref. [10] has been spread out evenly over $\Delta E = 30$ keV energy bins (visible as red line) to allow correlation with the B(GT$^-$) values from the (^{3}He,t) reaction.

The unusual spreading of the GT strength in the $A = 76$ system along with the apparent lack of correlation of GT$^+$ and GT$^-$ strength necessitates a thorough theoretical understanding. The situation is even more puzzling, since other $\beta\beta$ decaying nuclei not far away from $A = 76$, like ^{96}Zr or ^{100}Mo, exhibit a completely different behavior, where most of the low-energy GT$^+$ and GT$^-$ strength resides in a single transition, thereby making up most of the $\beta\beta$ decay matrix element [74]. At present, and also in following up on arguments given in Ref. [12] and more recently in Refs. [75,76], we can only suggest that rather specific structure effects pertaining to the particulars of the $A = 76$ system play the essential role. In fact, nuclei in the region of $A = 76$ are known to exhibit collective surface degrees of freedom, which make them susceptible to deformation into prolate, oblate or even triaxial shapes. In Refs. [77,78] several studies of GT strength values and $2\nu\beta\beta$ decay matrix elements in a deformed quasiparticle random phase approximation formalism (*deformed*-QRPA) are presented for a series of $\beta\beta$ decay partners. The authors show that the size of the $2\nu\beta\beta$ matrix elements depends critically on the overlap of the mother and the grand-daughter nuclear wave function. This overlap scales approximately as $exp[-(\Delta\beta_2)^2]$

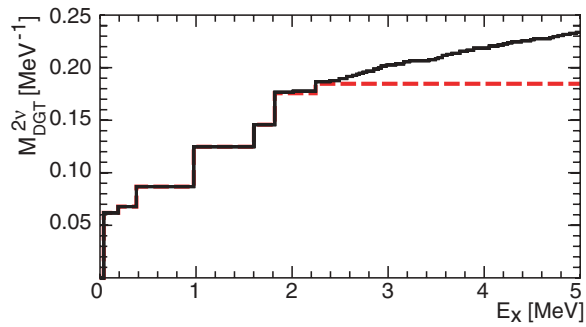

FIG. 8. (Color online) Running sum of the $2\nu\beta\beta$ matrix element $M^{2\nu}_{\rm DGT}$ with (solid line) and without (dashed line) the correlation of continuum B(GT$^+$) strength.

TABLE V. Evaluation of $2\nu\beta\beta$ decay matrix elements by correlating $B(\mathrm{GT}^+)$ values from a ^{76}Se(d,^{2}He) reaction [10] with $B(\mathrm{GT}^-)$ values from the present ^{76}Ge(^{3}He,t) reaction. Because of the different energy resolutions in these experiments, the $B(\mathrm{GT}^-)$ values from the levels falling into ≈120 keV resolution bin of the (d,^{2}He) reaction (in the curly brackets) have been summed. If each GT^+ strength were evenly distributed among the states appearing in the curly brackets, the summed matrix element would reduce slightly to 0.173 MeV^{-1}.

E_x[MeV] (d,^{2} He)	$B(\mathrm{GT}^+)$	E_x[MeV] (^{3}He, t)	$B(\mathrm{GT}^-)$	$M^{2\nu}_{\mathrm{DGT}}$ [MeV^{-1}]
0.04/0.08	0.102(13)	{0.086, 0.120}	0.153(16)	0.062(10)
0.50	0.066(12)	{0.265, 0.500}	0.055(18)	0.025(7)
1.03	0.076(11)	{1.022, 1.063, 1.098}	0.169(19)	0.038(7)
1.63	0.077(11)	{1.573, 1.637, 1.693, 1.718}	0.074(12)	0.021(5)
1.86	0.141(16)	{1.792, 1.852, 1.902, 1.929}	0.095(10)	0.030(5)
2.22	0.078(9)	{2.338}	0.019(2)	0.009(1)
				$\sum = 0.186(16)$

[77], where $\Delta\beta_2$ is the difference of the quadrupole deformation of the mother and grand-daughter nucleus. The sign of the deformation seems to be only of secondary importance. In Refs. [79,80] sub-barrier fusion processes have experimentally been studied in great detail at the Notre Dame tandem accelerator using ^{27}Al and ^{16}O projectiles on all stable Ge isotopes. A significant enhancement of the fusion cross section was observed when going from ^{70}Ge to ^{76}Ge, which was interpreted as due to a shape change from a rather spherical (or possibly slightly oblate) shape (^{70}Ge, ^{72}Ge) to a sizable prolate shape of ^{76}Ge. Esbenson [81] though, has reviewed this interpretation and arrives at slightly different conclusions on the basis of a more detailed theoretical treatment.

Unfortunately, similar experimental fusion studies on Se isotopes do not exist. However, in Ref. [82] theoretical calculations for ^{76}Ge and ^{76}Se are described using a *deformed*-QRPA. These authors show that with the Skyrme Sk3 interaction stable oblate deformations for ^{76}Se are obtained, though with a phenomenological deformed Woods-Saxon potential the system acquires a prolate configuration. Still, it is conceivable that the difference of the β_2 values of the two systems,^{76}Se and ^{76}Ge, is large.

Whereas a quenching of the GT type $\beta\beta$ decay matrix elements in cases of largely different shapes of the mother and the grand-daughter nucleus may be rather intuitive, it is still open, how shape degrees of freedom would manifest themselves in the single GT strength distributions. In Refs. [82–86] Sarriguren *et al*. have studied the effect of deformation and show that the GT strength distributions in cases of deformed nuclear shapes are significantly more fragmented than those of the corresponding spherical ones, which is interpreted as a result of a break down of the spherical shell degeneracy. It was also shown by Sarriguren *et al*. [85] that different deformations may even lead to sizable differences between the GT strength distributions, in particular when oblate and prolate shapes are simultaneously involved. In fact, as already suggested by Hamamoto and Zhang [87], one could possibly deduce the ground-state deformation by a comparison of the GT strength distribution with a theoretical model. A rather convincing example is the $A = 76$, $N = Z$ nucleus ^{76}Sr, where the low-energy GT distribution has recently been extracted from the β decay branches measured at CERN-ISOLDE [88]. The GT distribution clearly differentiates between prolate and oblate deformation and gives preference to a prolate shape.

The present experimental findings using charge-exchange reactions support the general picture of the nuclear shape dependence of GT strength distributions, though the experimentally observed differences and the apparent lack of correlation between GT^+ and GT^- strength seem to be even more pronounced than what theoretical calculations indicate. The GT type $\beta\beta$ decay nuclear matrix elements are likely affected by deformation, however, in how far the non-GT type matrix elements, which are mostly relevant for the neutrinoless decay, are affected as well, may still be a matter of a debate.

IV. CONCLUSION

We have presented the GT strength distribution obtained from a 420 MeV (^{3}He,t) experiment on the $\beta\beta$ decaying nucleus ^{76}Ge. Owing to the superb final state energy resolution of 30 keV, rather unexpected and even surprising features of the $A = 76$ system involved in the $\beta\beta$ decay have been unveiled. The low-energy (i.e., $E_x \leqslant 5$ MeV) GT^- strength distribution is found to be highly fragmented and distributed among about 70 individual states, whose angular distributions have all been analyzed. The extreme spreading of the GT^- distribution is in marked contrast to the GT^+ strength distribution observed in an earlier ^{76}Se(d,^{2}He) reaction at a 120 keV resolution leading to the same intermediate nucleus ^{76}As, where only five prominent states dominate the excitation-energy spectrum. An attempt was made to correlate the states populated from the two different directions and thereby construct the $2\nu\beta\beta$ matrix element. Despite a significant lack of correlation among the GT strength values from the two directions, we still conclude that the states at low excitation energies make up a substantial fraction of the full $2\nu\beta\beta$ matrix element. Contributions from the GT resonance are likely small and, if existent at all, one may suspect that phase cancelations among the contributing configurations prevent sizable total contributions. The extreme spreading of the GT^- strength and the apparent difference between the GT^+ and GT^- distribution was interpreted as an effect of deformation. This interpretation is supported by QRPA inspired models, where shape degrees of freedom are incorporated.

ACKNOWLEDGMENTS

We are indebted to Prof. S. Schönert (Technische Universitöt München) from the GERDA Collaboration for providing us with a small piece of enriched ^{76}Ge for the preparation of an appropriate target. We are most thankful to Dr. S. Nisi from the Gran Sasso National Laboratory for measuring the isotopic composition of the Ge target material using the ICP-MS facility. We thank the RCNP accelerator staff for their fine technical support during the course of the experiment. This work was partly supported by JSPS under Grant No. 22540310. The work was also partly financed by the Deutsche Forschungsgemeinschaft (DFG) under grant no. FR 601/3-1.

[1] B. D. Anderson, T. Chittrakarn, A. R. Baldwin, C. Lebo, R. Madey, P. C. Tandy, J. W. Watson, B. A. Brown, and C. C. Foster, Phys. Rev. C **31**, 1161 (1985).

[2] B. D. Anderson, T. Chittrakarn, A. R. Baldwin, C. Lebo, R. Madey, P. C. Tandy, J. W. Watson, C. C. Foster, B. A. Brown, and B. H. Wildenthal, Phys. Rev. C **36**, 2195 (1987).

[3] R. L. Helmer, Can. J. Phys. **65**, 588 (1987).

[4] W. P. Alford, R. L. Helmer, R. Abegg, A. Celler, D. Frekers, P. Green, O. Häusser, R. Henderson, K. Hicks, K. Jackson *et al.*, Nucl. Phys. A **514**, 49 (1990).

[5] B. D. Anderson, N. Tamimi, A. R. Baldwin, M. Elaasar, R. Madey, D. M. Manley, M. Mostajabodda'vati, J. W. Watson, W. M. Zhang, and C. C. Foster, Phys. Rev. C **43**, 50 (1991).

[6] C. D. Goodman, C. A. Goulding, M. B. Greenfield, J. Rapaport, D. E. Bainum, C. C. Foster, W. G. Love, and F. Petrovich, Phys. Rev. Lett. **44**, 1755 (1980).

[7] T. N. Taddeucci, C. A. Goulding, T. A. Carey, R. C. Byrd, C. D. Goodman, C. Gaarde, J. Larsen, D. Horen, J. Rapaport, and E. Sugarbaker, Nucl. Phys. A **469**, 125 (1987).

[8] K. P. Jackson, A. Celler, W. P. Alford, K. Raywood, R. Abegg, R. E. Azuma, C. K. Campbell, S. El-Kateb, D. Frekers, P. W. Green *et al.*, Phys. Lett. B **201**, 25 (1988).

[9] E.-W. Grewe, D. Frekers, S. Rakers, T. Adachi, C. Bäumer, N. T. Botha, H. Dohmann, H. Fujita, Y. Fujita, K. Hatanaka *et al.*, Phys. Rev. C **76**, 054307 (2007).

[10] E.-W. Grewe, C. Bäumer, H. Dohmann, D. Frekers, M. N. Harakeh, S. Hollstein, H. Johansson, L. Popescu, S. Rakers, D. Savran *et al.*, Phys. Rev. C **78**, 044301 (2008).

[11] C. J. Guess, T. Adachi, H. Akimune, A. Algora, Sam M. Austin, D. Bazin, B. A. Brown, C. Caesar, J. M. Deaven, H. Ejiri *et al.*, Phys. Rev. C **83**, 064318 (2011).

[12] H. Ejiri, Phys. Rep. **338**, 265 (2000).

[13] H. Ejiri, J. Phys. Soc. Jpn. **74**, 2101 (2005).

[14] H. T. Janka, K. Langanke, A. Marek, G. Martínez-Pinedo, and B. Müller, Phys. Rep. **442**, 38 (2007).

[15] K. Langanke and G. Martínez-Pinedo, Rev. Mod. Phys. **75**, 819 (2003).

[16] P. Vogel and M. R. Zirnbauer, Phys. Rev. Lett. **57**, 3148 (1986).

[17] A. Staudt, K. Muto, and H. V. Klapdor-Kleingrothaus, Europhys. Lett. **13**, 31 (1990).

[18] J. Suhonen and O. Civitarese, Phys. Rep. **300**, 123 (1998).

[19] E. Caurier, F. Nowacki, A. Poves, and J. Retamosa, Nucl. Phys. A **654**, 973c (1999).

[20] V. A. Rodin, A. Faessler, F. Šimkovic, and P. Vogel, Phys. Rev. C **68**, 044302 (2003).

[21] J. Suhonen, Phys. Lett. B **607**, 87 (2005).

[22] O. Civitarese and J. Suhonen, Phys. Lett. B **626**, 80 (2005).

[23] O. Civitarese and J. Suhonen, Nucl. Phys. A **761**, 313 (2005).

[24] V. A. Rodin, A. Faessler, F. Šimkovic, and P. Vogel, Nucl. Phys. A **766**, 107 (2006); Erratum **A793**, 213 (2007).

[25] E. Caurier, F. Nowacki, and A. Poves, Int. J. Mod. Phys. E **16**, 552 (2007).

[26] E. Caurier, J. Menéndez, F. Nowacki, and A. Poves, Phys. Rev. Lett. **100**, 052503 (2008).

[27] F. Šimkovic, A. Faessler, V. A. Rodin, P. Vogel, and J. Engel, Phys. Rev. C **77**, 045503 (2008).

[28] F. Šimkovic, A. Faessler, H. Müther, V. Rodin, and M. Stauf, Phys. Rev. C **79**, 055501 (2009).

[29] R. Madey, B. S. Flanders, B. D. Anderson, A. R. Baldwin, J. W. Watson, Sam M. Austin, C. C. Foster, H. V. Klapdor, and K. Grotz, Phys. Rev. C **40**, 540 (1989).

[30] A. A. Vasenko, I. V. Kirpichnikov, V. A. Kuznetsov, A. S. Starostin, A. G. Djanyan, V. S. Pogosov, S. P. Shachysiyan, and A. G. Tamanyan, Mod. Phys. Lett. A **5**, 1299 (1990).

[31] H. S. Miley, F. T. Avignone III, R. L. Brodzinski, J. I. Collar, and J. H. Reeves, Phys. Rev. Lett. **65**, 3092 (1990).

[32] F. T. Avignone III, R. Brodzinski, C. Guerard, I. Kirpichnikov, H. Miley, V. Pogosov, J. Reeves, A. Starostin, and A. Tamanyan, Phys. Lett. B **256**, 559 (1991).

[33] F. T. Avignone III, Prog. Part. Nucl. Phys. **32**, 223 (1994).

[34] A. Morales, Nucl. Phys. B, Proc. Suppl. **77**, 335 (1999).

[35] M. Günther, J. Hellmig, G. Heusser, M. Hirsch, H. Klapdor-Kleingrothaus, B. Maier, H. Päs, F. Petry, Y. Ramachers, H. Strecker *et al.*, Phys. Rev. D **55**, 54 (1997).

[36] H. V. Klapdor-Kleingrothaus, A. Dietz, L. Baudis, G. Heusser, I. V. Krivosheina, B. Majorovits, H. Paes, H. Strecker, V. Alexeev, A. Balysh *et al.*, Eur. Phys. J. **12**, 147 (2001).

[37] C. Dörr and H.V. Klapdor-Kleingrothaus, Nucl. Instrum. Methods Phys. Res. A **513**, 596 (2003).

[38] A. M. Bakalyarov, A. Y. Balysh, S. T. Belyaev, V. I. Lebedev, and S. V. Zhukov, Phys. Part. Nucl. Lett. **2**, 77 (2005); Pisma Fiz. Elem. Chastits At. Yadra **2**, 21 (2005).

[39] A. S. Barabash, Phys. Rev. C **81**, 035501 (2010).

[40] P. Peiffer, D. Motta, S. Schoenert, and H. Simgen, Nucl. Phys. B, Proc. Suppl. **143**, 511 (2005).

[41] C. E. Aalseth, D. Anderson, R. Arthur, F. T. Avignone III, C. Baktash, T. Ball, A. S. Barabash, F. Bertrand, R. L. Brodzinski, V. Brudanin *et al.*, Nucl. Phys. B, Proc. Suppl. **138**, 217 (2005).

[42] H. V. Klapdor-Kleingrothaus, I. V. Krivosheina, A. Dietz, and O. Chkvorets, Phys. Lett. B **586**, 198 (2004).

[43] H. V. Klapdor-Kleingrothaus and I. V. Krivosheina, Mod. Phys. Lett. A **21**, 1547 (2006).

[44] G. Douysset, T. Fritioff, C. Carlberg, I. Bergström, and M. Björkhage, Phys. Rev. Lett. **86**, 4259 (2001).

[45] G. Audi, A. H. Wapstra, and C. Thibault, Nucl. Phys. A **729**, 337 (2003).

[46] H. Primakoff and S. P. Rosen, Rep. Prog. Phys. **22**, 121 (1959).

[47] W. G. Love and M. A. Franey, Phys. Rev. C **24**, 1073 (1981).

[48] M. A. Franey and W. G. Love, Phys. Rev. C **31**, 488 (1985).

[49] H. Akimune, I. Daito, Y. Fujita, M. Fujiwara, M. Greenfield, M. Harakeh, T. Inomata, J. Jänecke, K. Katori, S. Nakayama *et al.*, Nucl. Phys. A **569**, 245 (1994).

[50] Y. Fujita, Y. Shimbara, A. F. Lisetskiy, T. Adachi, G. P. A. Berg, P. von Brentano, H. Fujimura, H. Fujita, K. Hatanaka, J. Kamiya *et al.*, Phys. Rev. C **67**, 064312 (2003).
[51] Y. Fujita, B. Rubio, and W. Gelletly, Prog. Part. Nucl. Phys. **66**, 549 (2011).
[52] M. Fujiwara, H. Akimune, I. Daito, H. Fujimura, Y. Fujita, K. Hatanaka, H. Ikegami, I. Katayama, K. Nagayama, N. Matsuoka *et al.*, Nucl. Instrum. Methods Phys. Res. A **422**, 484 (1999).
[53] T. Wakasa, K. Hatanaka, Y. Fujita, G. P. A. Berg, H. Fujimura, H. Fujita, M. Itoh, J. Kamiya, T. Kawabata, K. Nagayama *et al.*, Nucl. Instrum. Methods Phys. Res. A **482**, 79 (2002).
[54] Y. Fujita, K. Hatanaka, G. P. A. Berg, K. Hosono, N. Matsuoka, S. Morinobu, T. Noro, M. Sato, K. Tamura, and H. Ueno, Nucl. Instrum. Methods Phys. Res. B **126**, 274 (1997).
[55] H. Fujita, G. P. A. Berg, Y. Fujita, K. Hatanaka, T. Noro, E. J. Stephenson, C. C. Foster, H. Sakaguchi, M. Itoh, T. Taki *et al.*, Nucl. Instrum. Methods Phys. Res. A **469**, 55 (2001).
[56] H. Fujita, Y. Fujita, G. P. A. Berg, A. D. Bacher, C. C. Foster, K. Hara, K. Hatanaka, T. Kawabata, T. Noro, H. Sakaguchi *et al.*, Nucl. Instrum. Methods Phys. Res. A **484**, 17 (2002).
[57] T. Noro, M. Fujiwara, O. Kamigaito, S. Hirata, Y. Fujita, A. Yamagoshi, T. Takahashi, H. Akimune, Y. Sakemi, M. Yosoi *et al.*, RCNP Annual Report No.177 (1991).
[58] S. Nisi (private communication); internal note Feb-23-2012, Laboratori Nazionali del Gran Sasso, Servizio di Chimica e Impianti Chimici.
[59] J. F. Ziegler (2011) [http://www.srim.org].
[60] National Nuclear Data Center, Brookhaven National Laboratory (2012), URL [http://www.nndc.bnl.gov].
[61] M.A. Hofstee, S. Y. van der Werf, A. M. van den Berg, N. Blasi, J. A. Bordewijk, W. T. A. Borghols, R. De Leo, G. T. Emery, S. Fortier, S. Galès *et al.*, Nucl. Phys. A **588**, 729 (1995).
[62] J. Cook and J. A. Carr, computer program FOLD, Florida State University, unpublished (1988), based on F. Petrovich and D. Stanley, Nucl. Phys. A **275**, 487 (1977), modified as described in J. Cook, K. W. Kemper, P. V. Drumm, L. K. Fifield, M. A. C. Hotchkis, T. R. Ophel, and C. L. Woods, Phys. Rev. C **30**, 1538 (1984) and R. G. T. Zegers, S. Fracasso and G. Colò, NSCL, Michigan State University, unpublished (2006).
[63] R. G. T. Zegers, H. Akimune, Sam M. Austin, D. Bazin, A. M. van den Berg, G. P. A. Berg, B. A. Brown, J. Brown, A. L. Cole, I. Daito *et al.*, Phys. Rev. C **74**, 024309 (2006).
[64] M. Rashdan, Eur. Phys. J. **16**, 371 (2003).
[65] J. Kamiya, K. Hatanaka, T. Adachi, K. Fujita, K. Hara, T. Kawabata, T. Noro, H. Sakaguchi, N. Sakamoto, Y. Sakemi *et al.*, Phys. Rev. C **67**, 064612 (2003).
[66] S. Y. van der Werf, S. Brandenburg, P. Grasduk, W. A. Sterrenburg, M. N. Harakeh, M. B. Greenfield, B. A. Brown, and M. Fujiwara, Nucl. Phys. A **496**, 305 (1989).
[67] P. Puppe, D. Frekers, T. Adachi, H. Akimune, N. Aoi, B. Bilgier, H. Ejiri, H. Fujita, Y. Fujita, M. Fujiwara *et al.*, Phys. Rev. C **84**, 051305(R) (2011).
[68] G. Perdikakis, R. G. T. Zegers, Sam M. Austin, D. Bazin, C. Caesar, J. M. Deaven, A. Gade, D. Galaviz, G. F. Grinyer, C. J. Guess *et al.*, Phys. Rev. C **83**, 054614 (2011).
[69] D. Frekers, H. Ejiri, H. Akimune, T. Adachi, B. Bilgier, B. A. Brown, B. T. Cleveland, H. Fujita, Y. Fujita, M. Fujiwara *et al.*, Phys. Lett. B **706**, 134 (2011).
[70] K. Nakamura *et al.* (Particle Data Group), J. Phys. G: Nucl. Part. Phys. **37**, 075021 (2010).
[71] H. Ejiri, Nucl. Phys. A **577**, 399 (1994).
[72] H. Ejiri and H. Toki, J. Phys. Soc. Jpn. **65**, 7 (1996).
[73] M. Ericson, T. Ericson, and P. Vogel, Phys. Lett. B **328**, 259 (1994).
[74] D. Frekers, *Workshop on Calculation of Double-Beta Decay Matrix Elements*, Prague [AIP Conf. Proc. **1190**, 40 (2009)].
[75] H. Ejiri, J. Phys. Soc. Jpn. **78**, 074201 (2009).
[76] H. Ejiri, J. Phys. Soc. Jpn. **81**, 033201 (2012).
[77] F. Šimkovic, L. Pacearescu, and A. Faessler, Nucl. Phys. A **733**, 321 (2004).
[78] R. Álvarez-Rodríguez, P. Sarriguren, E. Moya de Guerra, L. Pacearescu, A. Faessler, and F. Šimkovic, Phys. Rev. C **70**, 064309 (2004).
[79] E. F. Aguilera, J. J. Vega, J. J. Kolata, A. Morsad, R. G. Tighe, and X. J. Kong, Phys. Rev. C **41**, 910 (1990).
[80] E. F. Aguilera, J. J. Kolata, and R. J. Tighe, Phys. Rev. C **52**, 3103 (1995).
[81] H. Esbensen, Phys. Rev. C **68**, 034604 (2003).
[82] P. Sarriguren, E. Moya de Guerra, L. Pacearescu, A. Faessler, F. Šimkovic, and A. A. Raduta, Phys. Rev. C **67**, 044313 (2003).
[83] P. Sarriguren, E. Moya de Guerra, A. Escuderos, and A. C. Carrizo, Nucl. Phys. A **635**, 55 (1998).
[84] P. Sarriguren, E. Moya de Guerra, and A. Escuderos, Nucl. Phys. A **658**, 13 (1999).
[85] P. Sarriguren, E. Moya de Guerra, and A. Escuderos, Nucl. Phys. A **691**, 631 (2001).
[86] P. Sarriguren, E. Moya de Guerra, and A. Escuderos, Phys. Rev. C **64**, 064306 (2001).
[87] I. Hamamoto and X. Z. Zhang, Z. Phys. A **353**, 145 (1995).
[88] E. Nácher, A. Algora, B. Rubio, J. L. Taín, D. Cano-Ott, S. Courtin, P. Dessagne, F. Maréchal, C. Miehé, E. Poirier *et al.*, Phys. Rev. Lett. **92**, 232501 (2004).